



**HAL**  
open science

## Anticancer properties of lipid and poly( $\epsilon$ -caprolactone) nanocapsules loaded with ferrocenyl-tamoxifen derivatives

Feten Najlaoui, Pascal Pigeon, Sonia Aroui, Mylène Pezet, Lucie Sancey, Naziha Marrakchi, Ali Rhouma, Gérard Jaouen, Michel de Waard, Benoît Busser, et al.

### ► To cite this version:

Feten Najlaoui, Pascal Pigeon, Sonia Aroui, Mylène Pezet, Lucie Sancey, et al.. Anticancer properties of lipid and poly( $\epsilon$ -caprolactone) nanocapsules loaded with ferrocenyl-tamoxifen derivatives. *Journal of Pharmacy and Pharmacology*, 2018, 70 (11), pp.1474-1484. 10.1111/jphp.12998 . hal-01861749

**HAL Id: hal-01861749**

**<https://hal.science/hal-01861749>**

Submitted on 5 Nov 2018

**HAL** is a multi-disciplinary open access archive for the deposit and dissemination of scientific research documents, whether they are published or not. The documents may come from teaching and research institutions in France or abroad, or from public or private research centers.

L'archive ouverte pluridisciplinaire **HAL**, est destinée au dépôt et à la diffusion de documents scientifiques de niveau recherche, publiés ou non, émanant des établissements d'enseignement et de recherche français ou étrangers, des laboratoires publics ou privés.

1 **Anticancer properties of lipid and poly( $\epsilon$ -caprolactone) nanocapsules loaded with**  
2 **ferrocenyl tamoxifen derivatives**

3 Feten Najlaoui<sup>1,2</sup>, Pascal Pigeon (PhD)<sup>3,4</sup>, Sonia Aroui (PhD)<sup>5</sup>, Mylène Pezet<sup>6</sup> (PhD), Lucie Sancey  
4 (PhD)<sup>6</sup>, NazihaMarrakchi (Professor)<sup>1</sup>, Ali Rhouma (Professor)<sup>7</sup>, Gérard Jaouen (Professor)<sup>3,4</sup>, Michel  
5 De Waard (PhD)<sup>8</sup>, Benoit Busser (PharmD, PhD)<sup>6</sup>, Stéphane Gibaud (PharmD, PhD)<sup>2</sup>  
6

7 <sup>1</sup>Laboratoire des Venins et Biomolécules Thérapeutiques LR11IPT08, Institut Pasteur de Tunis, 13, Place  
8 Pasteur, 1002 Tunis, Tunisia.

9 <sup>2</sup>Université de Lorraine, EA 3452/CITHEFOR, 5 rue Albert Lebrun (Faculté de Pharmacie), F-54000 Nancy,  
10 France.

11 <sup>3</sup>Chimie ParisTech, 11 rue Pierre et Marie Curie, Paris F75231 Paris Cedex 05, France.

12 <sup>4</sup>Sorbonne Universités, UPMC Université Paris 6, Institut Parisien de Chimie Moléculaire (IPCM) – UMR 8232,  
13 4 place Jussieu, 75252 Paris Cedex 05, France.

14 <sup>5</sup>Laboratory of Biochemistry, Molecular Mechanisms and Diseases Research Unit, UR12ES08, Faculty of  
15 Medicine, University of Monastir.

16 <sup>6</sup>University Grenoble Alpes, IAB Inserm U1209 / CNRS UMR 5309, Grenoble University Hospital, F-38000  
17 Grenoble, France.

18 <sup>7</sup>Research Unit of Plant Protection and Environment, Olive Tree Institute, Mahrajene City BP 208, 1082 Tunis,  
19 Tunisia

20 <sup>8</sup>Institut du Thorax, INSERM UMR 1087 / CNRS UMR 6291, 8 quai Moncousu, Nantes University, Labex Ion  
21 Channels, Science & Therapeutics, 44007 Nantes Cedex 1, France.

22

23 **Author to whom correspondence should be sent:**

24 Stéphane Gibaud - Université de Lorraine, EA 3452/CITHEFOR - 5, rue Albert Lebrun  
25 (Faculté de Pharmacie) - F-54000 Nancy, France; Tel : +33 3 72 74 73 06; Mobile : +33 6 68  
26 47 4 00; email: stephane.gibaud@univ-lorraine.fr

27

28 **Abstract**

29 **Objective:** We synthesized new tamoxifen derivatives as anticancer drug candidates and  
30 elaborated on convection-enhanced delivery (CED) as strategy for delivery.

31 **Methods:** To overcome the issue of their poor solubility, these ferrocenyl-tamoxifen  
32 derivatives were esterified and encapsulated into different nanocarriers, i.e lipid (LNC) and  
33 polymeric nanocapsules (PNL-NC). We describe the chemistry, the encapsulation and the  
34 physicochemical characterization of these formulations.

35 **Key findings:** Starting compounds [phthalimido-ferrocidiphenol and succinimido-  
36 ferrocidiphenol], esterified prodrugs and their nanocapsules formulations were characterized.  
37 These drug candidates displayed a strong *in vitro* activity against breast and glioblastoma  
38 cancer cells. The ester prodrugs were toxic for glioblastoma cells ( $IC_{50} = 9.2 \times 10^{-2} \mu M$  and  
39  $6.7 \times 10^{-2} \mu M$  respectively). The  $IC_{50}$  values for breast cancer cells were higher for these  
40 compounds.

41 The encapsulation of the esterified compounds in LNCs ( $\approx 50$  nm) or PCL-NCs ( $\approx 300$  nm)  
42 did not prevent their efficacy on glioblastoma cells. These anticancer effects were due to both  
43 a blockade in the S-phase of the cell cycle and apoptosis. Moreover, the tamoxifen  
44 derivatives-loaded nanocapsules induced no toxicity for healthy astrocytes and showed no  
45 hemolytic properties. Loaded Lipid Nanocapsules (LNC) presented interesting profiles for the  
46 optimal delivery of active compounds.

47 **Conclusion:** Phthalimido- and Succinimido-esters represent an innovative approach to treat  
48 cancers with cerebral localizations such as glioblastoma or brain metastases from breast  
49 cancers.

50

51 **Keywords (5):** Lipid nanocapsules, polymer nanocapsules, ferrocenyl tamoxifen  
52 derivatives, breast cancer, glioblastoma.

## 53 1. Introduction

54 Tamoxifen has been used for endocrine therapy to treat breast cancer for many years. This  
55 selective estrogen receptor modulator (SERM) possesses an active metabolite named  
56 hydroxytamoxifen that competitively binds to estrogen receptor (ER) and thus inhibits cancer  
57 cell proliferation.<sup>[1]</sup> Nonetheless, tamoxifen efficacy is only observed against estrogen  
58 receptor-positive tumors (ER<sup>+</sup>), but resistance occurs after long-term usage.<sup>[2]</sup> Importantly,  
59 tamoxifen is also able to treat other cancers, such as glioblastoma, in association with the  
60 standard of care, which is temozolomide.<sup>[3]</sup> The embedding of a ferrocenyl unit into the  
61 tamoxifen skeleton can lead to a new family of breast cancer drug candidates named  
62 hydroxyferrocifens.<sup>[4,5]</sup> Hydroxyferrocifens have the advantage of dual functionality.  
63 Effectively, these molecules have endocrine-modulating properties along with cytotoxic  
64 activities. A variety of hydroxyferrocifens were synthesized by structure-reactivity  
65 relationship studies.<sup>[6]</sup> The activity remains when the dimethylaminoalkyl chain, which is  
66 inherited from the hydroxytamoxifen, is suppressed, leading to the ferrocidiphenol series.  
67 Among this series, some compounds with modification at the ethyl group, that is also  
68 inherited from hydroxytamoxifen, had better activity, in particular when a polar group was  
69 fixed at the end of the alkyl chain.<sup>[7,8]</sup> Thus, the introduction of a polar imide group gave rise  
70 to ferrocidiphenol (Ferr) compounds, namely phthalimido-ferrocidiphenol (PhtFerr)  
71 (C<sub>35</sub>H<sub>29</sub>FeNO<sub>4</sub>) and succinimido-ferrocidiphenol (SuccFerr) (C<sub>31</sub>H<sub>29</sub>FeNO<sub>4</sub>), that were found  
72 to be very effective on breast cancer cells (MDA-MB-231) and, more surprisingly, on human  
73 glioblastoma cancer cells (U87).<sup>[9]</sup> The mechanism underlying the Ferr cytotoxicity is only  
74 partly understood. Previous *in vitro* studies demonstrated that at least some Ferr metabolites  
75 produced in the cell are electrophilic quinonemethides that can induce growth arrest with

76 senescence and apoptosis phenomena.<sup>[10,11]</sup> Recently, adducts of these quinonemethides with  
77 compounds bearing thiol functional group, as models of some cellular nucleophiles were  
78 identified.<sup>[12]</sup>

79 Metal-based anticancer drugs, such as PhtFerr and SuccFerr, are very hydrophobic  
80 compounds that cannot be formulated in aqueous solutions easily.<sup>[13]</sup> Therefore, we both  
81 synthesized their respective ester prodrugs Phtester and Succester and also encapsulated them  
82 into nanocarriers to overcome the issue of their poor solubility. We compared two different  
83 formulations, *ie* lipid nanocapsules (LNCs) and poly( $\epsilon$ -caprolactone) nanocapsules (PCL-  
84 NCs), for encapsulation efficiency and release of the prodrugs of interest. These nanocapsules  
85 can be considered as platforms for a future development but, in a first step, they could be  
86 administered locally by Convection-Enhanced Delivery (CED).

87 LNCs (~100 nm) have a special structure between those of polymer nanocapsules and  
88 liposomes. These particles have various advantages, including a solvent-free manufacturing  
89 process and a prolonged physical stability of more than 18 months.<sup>[14]</sup> Moreover, they allow  
90 the transport of multiple types of drugs, including lipophilic anticancer drugs such as  
91 paclitaxel, docetaxel, doxorubicin, hydroxytamoxifen, and etoposide;<sup>[15]</sup> DNA and small  
92 interfering RNAs;<sup>[16,17]</sup> radionuclides;<sup>[18,19]</sup> and nuclease-resistant locked nucleic acids,<sup>[20]</sup>  
93 offering a pharmaceutical solution for their parenteral administration.

94

95 PCL-NCs are larger vesicular systems (~300 nm) in which a lipophilic drug can be dissolved  
96 in an oily core and surrounded by a polymeric shell, allowing the drug to be absorbed onto the  
97 surface or entrapped within the nanocarriers.<sup>[21]</sup> Some of the advantages of polymeric  
98 nanocapsules are their high loading capacity for lipophilic drugs, the protection they provide

99 against enzymatic degradation and their physicochemical stability. Moreover, PCL is a  
100 polyester polymer that is biodegradable and biocompatible.<sup>[22]</sup> PCL is also considered a well-  
101 tolerated nanocarrier with very slow degradation.<sup>[23]</sup> It was recently used as a safe scaffold for  
102 brain delivery of therapeutic agents.<sup>[24]</sup> This paper details the physicochemical  
103 characterization of PhtFerr and SuccFerr and the synthesis of their respective esterified-  
104 derivatives Phtester and Succester. All of these compounds were loaded into LNCs and PCL-  
105 NCs. We studied the *in vitro* drug release profile of the encapsulated prodrugs and their  
106 cytotoxicity against glioblastoma U87 cell lines and human breast MDA-MB-231 cancer (this  
107 latter cell line is known to be very sensitive to ferrocenylphenols). All these novel tamoxifen  
108 derivatives were more toxic for cancer cells compared to the parent drug tamoxifen, but less  
109 toxic for normal astrocytes. The strong and promising anticancer effect was demonstrated by  
110 both an efficient blockade of the cell cycle and also proapoptotic activity in breast and  
111 glioblastoma cancer cells.

112

## 113 **2. Material and Methods**

### 114 **2.1. Chemistry**

115 Reagents, molecules and chemical reactions are described in the supplementary material S1.

116 The synthesis of PhtFerr and compound X have been previously described.<sup>[9]</sup>

117 The complete chemical synthesis is detailed in S1. Measurements of the octanol/water  
118 partition coefficient (log Po/w) were made using high-performance liquid chromatography  
119 (HPLC) according to a method described previously.<sup>[25]</sup>

120

### 121 **2.2. Solubility studies**

122 Unless otherwise specified, all of the solvents were obtained from either Gattefossé (Nanterre,  
123 France) or Sigma Aldrich (Saint Quentin Fallavier, France).

124 The solubility of Phtester and Succester was determined as follows: two milliliters of each  
125 vehicle was added to screw-cap vials containing an excess of each of the Phtester and  
126 Succester compounds (*ie* 500 mg). The mixture was heated in a shaking water bath  
127 (Memmert, Schwabach, Deutschland; 25°C, 48 h, 60 strokes/min) to improve the dissolution.  
128 When equilibrium was achieved, the mixture was centrifuged at 1400 × g for 5 min, and the  
129 undissolved powder was discarded. Concentrations were determined by HPLC.

130

### 131 **2.3. Preparation and loading of lipidic nanocapsules (LNC)**

132 Phtester-LNCs and Succester-LNCs were prepared by a one-step process based on a phase-  
133 inversion temperature method described elsewhere.<sup>[26]</sup> To obtain LNCs, Solutol® HS15 (17%  
134 w/w), Lipoid® S75 (1.5% w/w, Lipoid Kosmetic, Grasse, France), Labrafac® (18.3% w/w),

135 Phtester or Succester (1.7%), NaCl (1.75% w/w) and water (59.75% w/w) were mixed and  
136 heated under magnetic stirring up to 85°C. Three cycles of progressive heating and cooling  
137 between 85°C and 60°C were then carried out and followed by an irreversible shock induced  
138 by dilution with 2°C deionized water (45 or 70% v/v) added to the mixture when it had  
139 reached 70–75°C. The resulting suspension was passed through a 0.2 µM filter to remove the  
140 free drug. The drug candidate load was expressed as the weight of drug in the lipid phase (in  
141 mg/g; after freeze-drying). The encapsulation yield (in %) was the amount of drug obtained at  
142 the end of the process divided by the initial amount of drug.

143

#### 144 **2.4. Preparation and loading of polymeric nanocapsules (PCL-NCs)**

145 Phtester PCL-NCs and Succester PCL-NCs were prepared by a nanoprecipitation method that  
146 consisted of dissolving the molecules of interest (*ie* Phtester or Succester) in an organic phase:  
147 1% triethyl citrate (with 5 mg/mL of PhtFerr or Succester), 10% alcoholic solution of lecithin  
148 (5 mg of lecithin/mL, Sigma Aldrich, Saint Quentin Fallavier, France) and 89% solution of  
149 PCL in acetone (1% of PCL, Sigma Aldrich, Saint Quentin Fallavier, France). This organic  
150 phase (10 mL) was added drop-wise under magnetic stirring to an aqueous solution of 10%  
151 Pluronic F68 (20 mL). Acetone and a portion of the water were then removed by evaporation  
152 in a vacuum at +40°C (Rotavapor Heidolf 94200) to reach a final volume of 15 mL. PCL-NCs  
153 were then purified on a gel column (ACA Ultrogel<sup>®</sup> 54, Sigma Aldrich, Saint Quentin  
154 Fallavier, France). The drug candidate load was expressed as the weight of drug after freeze-  
155 drying (in mg/g of dried nanocapsules). The encapsulation yield (in %) was the amount of  
156 drug obtained after purification divided by the initial amount of drug.

157



158

## 159 **2.5. Freeze-drying of nanocapsules**

160 The samples were frozen in liquid nitrogen and freeze-dried (Labconco Freezone 6L). The  
161 temperature of each sample was equilibrated at -20 °C for 72 h. After lyophilisation, the  
162 samples were stored at -20°C until further use.

163

## 164 **2.6. Nanoparticles size and *zeta* potential**

165 The size and *zeta* potential distribution of the nanocarriers were analyzed using a Malvern  
166 Zetasizer® Nano Series DTS 1060 (Malvern Instruments S.A., Worcestershire, UK) operating  
167 at an angle of 90° and a temperature of 25°C (n=3). The nanocarriers were diluted 1:100 (v/v)  
168 in deionized water to ensure good scatter intensity on the detector. The *zeta* potential (n=3)  
169 was measured at pH 7.1 at 25°C at the same dilution using the following specifications:  
170 medium viscosity = 0.91 cP; refractive index (RI) = 1.33.

171

## 172 **2.7. Drug payload in nanocarriers and encapsulation efficiency**

173 Nanocarriers were first dissolved in acetonitrile. Then, the payload and encapsulation  
174 efficiency of LNCs and PCL-NCs were measured using an HPLC protocol. Twenty  
175 microliters of sample was injected into a C<sub>18</sub> column (Nucleosil®, 5 µm, 0.46 mm, 25 cm;  
176 Macherey Nagel, Eckbolsheim, France) using an autosampler (Spectra Physics AS1000). The  
177 mobile phase was a mixture of acetonitrile and water (65:35, v/v) with a flow rate of 1.5  
178 mL/min (Spectra Physics P1000XR; Thermo Electron S.A., Courtaboeuf, France). UV  
179 spectrophotometry was used to detect absorbance at 254 nm (Spectra Physics UV1000), and  
180 the peak area was used for quantification.

181

## 182 **2.8. *In vitro* drug release from nanocarriers**

183 The dialysis method was used as follows. Five milligrams of the lyophilized Phtester PCL-  
184 NCs, Succester PCL-NCs, Phtester LNCs, Succester LNCs, or Succester powder or  
185 Phtester powder were poured into 2 ml of 1% Tween<sup>®</sup> 20 and then transferred to a dialysis  
186 bag (molecular weight cutoff 14 kDa, Spectra/Por, Spectrum Laboratories, Paris, France).  
187 Each bag was placed into a bath of 498 mL of 1% Tween<sup>®</sup> 20 (pH 6.8). These preparations  
188 were placed in a bath shaking at 200 strokes/min at 25°C (Heito, France). One milliliter  
189 aliquots were taken at various intervals during the release period (24 h) and analyzed by  
190 HPLC to assess their drug content. The results are presented as the mean  $\pm$  standard  
191 deviation (SD) of 3 experiments.

192

### 193 **2.9. *In vitro* cytotoxicity**

194 The cytotoxic activity of Phtester LNCs, Phtester PCL-NCs, Succester LNCs, Succester  
195 PCL-NCs, Phtester, Succester, PhtFerr and SuccFerr was assessed using healthy astrocytes,  
196 the U87 human glioblastoma cell line and the human breast cancer (MDA-MB-231) cell  
197 line. Purified newborn rat primary astrocytes were obtained by mechanical dissociation  
198 from cultures of cerebral cortex (authorization n° 2015.080410145453v3) as previously  
199 described.<sup>[27]</sup> Fisher male rats were obtained from Charles River Laboratories France  
200 (L'Arbresle, France).

201 The U87 and MDA-MB-231 cell lines were obtained from ATCC (Molsheim, France).

202 The cells were grown at 37 °C/5% CO<sub>2</sub> in Dulbecco's modified Eagle medium (DMEM)  
203 (Invitrogen<sup>™</sup>, Life Technologies, Carlsbad, MA, USA) with glucose and L-glutamine  
204 (Cergy-Pontoise, France), 10% fetal calf serum (FCS) (BioWhittaker) and 1% antibiotic  
205 and antimycotic solution (Sigma, Saint-Quentin Fallavier, France). Phtester and Succester  
206 were dissolved in 1% dimethylsulfoxide (DMSO), whereas Phtester PCL-NCs, Phtester

207 LNCs, Succester LNCs, Succester PCL-NCs, blank LNCs and blank PCL-NCs were  
208 dispersed directly in DMEM. Tamoxifen was tested as a control drug.

209 All of the cells were seeded in sterile 96-well plates for 12 h with 100  $\mu$ L of medium  
210 ( $5 \times 10^3$ /well). Cells were then exposed to varying amounts of the indicated drug candidates  
211 at concentrations ranging from  $10^{-3}$  to  $10^{-9}$  M for 96 h at 37 °C. Blank nanocarriers were  
212 tested at an equivalent excipient concentration (compared to Phtester- or Succester-loaded  
213 PCL-NCs or LNCs). Cell cytotoxicity was then measured by a colorimetric assay using 3-  
214 (4,5-dimethylthiazol-2-yl)-2,5-diphenyltetrazolium bromide (MTT). Ninety microliters of  
215 DMEM medium with 10% MTT was added to each well and incubated for 2-4 h at 37 °C.  
216 MTT was removed, followed by addition of solubilizing solution (100  $\mu$ L DMSO),  
217 resulting in crystalline formazan formation. The absorbance was measured at 560 nm using  
218 a Beckman Coulter™ AD340S spectrophotometer. The absorbance is proportional to the  
219 number of viable cells, and survival was calculated as a percentage of the values measured  
220 for untreated cells.

221

## 222 **2.10. Cell cycle analysis**

223 In 6-well culture plates,  $5 \times 10^5$  U87 cells were seeded in 6-well culture plates with 2 mL of  
224 medium per well. After 12 h, the culture medium was removed, and cells were treated with  
225 10  $\mu$ M of Phtester PCL-NCs, Phtester LNCs, Succester PCL-NCs, Succester LNCs, Phtester,  
226 Succester, PhtFerr, SuccFerr or blank formulations (PCL-NCs and LNCs); the culture plates  
227 were incubated for 96 h at 37 °C. At the end of the experiment, cells were trypsinized, washed  
228 twice with PBS (without  $\text{Ca}^{2+}$  and  $\text{Mg}^{2+}$ ) and incubated with cold ethanol overnight at 4 °C.  
229 Cells were then centrifuged, washed once with PBS and then incubated with 0.5 mL PI/RNase  
230 (30 min, in the dark). The cell cycle was analyzed with an Accuri C6 flow cytometer (BD

231 Biosciences) in at least three independent experiments, with 50,000 cells being measured in  
232 each sample, and data were analyzed by FCS Express 5 Software (De Novo Software, USA).

233

### 234 **2.11. Cell apoptosis assay**

235 The U87 cell line was incubated with 10  $\mu$ M of different compounds (Phtester PCL-NCs,  
236 Phtester LNCs, Succester-PCL-NCs, Succester LNCs, Phtester, Succester, PhtFerr, or  
237 SuccFerr) for 96 h. Apoptotic cell death was revealed by flow cytometry using a  
238 phycoerythrin-conjugated monoclonal active caspase-3 antibody kit (BD Pharmingen, Le  
239 Pont de Claix, France) following the manufacturer's instructions. The cells were analyzed  
240 with a BD-Accuri C6 flow cytometer, and the data were analyzed by FCS Express 5  
241 Software. The percentage of apoptosis was obtained comparing it with the positive control

242

### 243 **2.12. Statistical analysis**

244 Statistical analyses were performed using GraphPad Prism 6 software (GraphPad Prism, La  
245 Jolla, USA). Kruskal–Wallis test (nonparametric) was used for cell cultures. Dunn's post-test  
246 (nonparametric) was then used for multiple comparisons. Mann and Whitney test was used to  
247 compare the release of the complexes for each formulation.

248

## 249 **3. Results**

250

### 251 **3.1. Chemistry**

252 PhtFerr and SuccFerr were synthesized by substitution of the chlorine atom of 5-chloro-2-  
253 ferrocenyl-1,1-bis-(4-hydroxyphenyl)-pent-1-ene (compound X) with an imide (succinimide,  
254 Figure 1 and S1). The ester prodrugs (N-{4-ferrocenyl-5,5-bis-(4-acetoxyphenyl)-pent-4-  
255 enyl}phthalimide Phtester) and (N-{4-ferrocenyl-5,5-bis-(4-acetoxyphenyl)-pent-4-  
256 enyl}succinimide Succester) were obtained by acetylation of PhtFerr and SuccFerr,  
257 respectively (Figure 1). The characterization of the products is in supplementary materials S1.

258

### 259 **3.2. Solubility studies**

260 To find the optimal formulation of LNCs and PCL-NCs, we tested the dissolution properties  
261 of various surfactants [Solutol<sup>®</sup> HS 15 (polyoxyethylated 12-hydroxystearic acid),  
262 triethylcitrate, Capryol<sup>®</sup> 90 (propylene glycol monocaprylate), Transcutol<sup>®</sup> HP (highly  
263 purified diethylene glycol monoethyl ether), Labrasol<sup>®</sup> ALF (caprylocaproyl polyoxyl-8  
264 glycerides), Maisine<sup>®</sup> 35-1 (glycerol monolinoleate), Miglyol<sup>®</sup> 812 (caprylic/capric  
265 triglyceride, Dynamit Nobel, Leverkusen, Germany), Labrafac<sup>®</sup> (medium-chain triglycerides),  
266 Tween<sup>®</sup> 20 (polysorbate 20), Tween<sup>®</sup> 80 (polysorbate 80)] and oils [olive oil, benzylbenzoate,  
267 ethyl oleate, Captex<sup>®</sup> 355 (glyceryltricaprylate/tricaprate), Triacetin (1,2,3-  
268 triacetoxyp propane)].

269

270 The results of solubility studies are reported in Table 1. Among the surfactants, Solutol<sup>®</sup>  
271 HS15 and Lafrac<sup>®</sup>, usually used to make LNCs, have very good solubilization capacities.

272 Triethylcitrate, which has previously been used to make PCL-NCs, has quite similar  
273 properties. Finally, Tween<sup>®</sup> 20 was used for solubility experiments.

274 In each formulation (*ie*, LNCs or PCL-NCs), the ferrocenyl-tamoxifen derivatives were  
275 dissolved in oily droplets. Surfactants were used to increase the solubility of both Phtester and  
276 Succester.

277

### 278 **3.3. Preparation and characterization of Phtester- and Succester-loaded nanocarriers**

279 Because Labrafac<sup>®</sup> and Solutol<sup>®</sup> HS15 were included in the formulation of LNCs,<sup>[26]</sup> the  
280 dissolutions of the drug candidates were very easy.

281 By mixing Phtester or Succester with excipients (*ie*, Labrafac<sup>®</sup>, Solutol<sup>®</sup> HS15 or Lipoid<sup>®</sup>) at  
282 well-characterized concentrations described by a ternary diagram<sup>[26]</sup> and by applying the  
283 phase-inversion process, Phtester LNCs and Succester LNCs were obtained. Their size ranges  
284 were very narrow with diameters between  $53.4 \pm 0.9$  nm and  $57.8 \pm 2.0$  nm (before  
285 lyophilisation), respectively, depending on the anticancer drug candidates payload  
286 (polydispersity index (PI) < 0.15) (Table 2). There was no significant difference before and  
287 after lyophilisation. Phtester LNCs and Succester LNCs were also characterized in terms of  
288 surface charge: *zeta* potential values were  $-10.8 \pm 2.0$  and  $-11.1 \pm 1.3$  mV, respectively.  
289 These physicochemical properties (Table 2) were very similar to those of the previously  
290 studied standard blank LNCs.<sup>[28,29]</sup> Indeed, because of the presence of PEG dipoles in their  
291 shells, 50-nm blank LNCs have a low *zeta* potential of approximately  $-10$  mV.<sup>[30]</sup> The  
292 possible presence of the active drug on the surface did not affect the *zeta* potential values,  
293 which suggests that Phtester and Succester were efficiently encapsulated in the LNCs. Like  
294 many other hydrophobic drugs,<sup>[31-33]</sup> both compounds were mostly encapsulated in the LNCs  
295 with a high encapsulation yields above 92% (Table 2).

296 Phtester PCL-NCs and Succester PCL-NCs were obtained by nanoprecipitation. They had  
297 sizes of  $303 \pm 12$  nm and  $295 \pm 18$  nm, respectively, that were similar to the size of the blank  
298 ones ( $289 \pm 7$  nm). The PCL-NCs loaded with Phtester and Succester exhibited negative  
299 charges of  $-18.2 \pm 0.7$  mV and  $-14.9 \pm 2.4$  mV, respectively. The incorporation of Phtester  
300 and Succester in PCL-NCs was very effective, as demonstrated by the high encapsulation  
301 yield and the *zeta* potential (Table 2).

302

### 303 **3.4. Pharmaceutical properties**

#### 304 **3.4.1. *In vitro* release study**

305 Phtester and Succester release studies were performed by a dialysis method. Under our  
306 conditions, the solubility of Phtester and Succester in the external compartment  
307 (Tween<sup>®</sup> 20, 1%) was 0.036 mg and 0.041 mg, respectively. The loaded LNC and PCL-NC  
308 formulations were both studied. Figure 2 illustrates the dissolution profiles obtained. Phtester  
309 PCL-NCs and Succester PCL-NCs were the most efficient formulations for effective drug  
310 release of greater than 70% after 12 h, whereas the diffusion from Phtester LNCs, Phtester,  
311 Succester-LNCs and Succester were quite slow, reaching only 30-40% release of the loaded  
312 drug candidates in the external phase after 24 h.

313

314

315

### 316 3.4.2. *In vitro* cytotoxicity on U87 cell lines

317 We performed MTT assays to evaluate the influence of the drug candidates on the viability of  
318 healthy astrocytes, MDA-MB-231 cells and U87 cells after treatment with Phtester- and  
319 Succester-loaded nanocapsules. A solution of 1% DMSO did not show any sign of toxicity.  
320 Therefore, the negative control was composed of the DMSO solution used to dissolve Phtester  
321 and Succester, and the corresponding viability was considered to be 100%. The blank  
322 formulations (nanocarriers alone) were non-toxic to breast cancer and glioblastoma cells and  
323 normal astrocytes in the micromolar range, as indicated in Table 3; the toxicity of tamoxifen  
324 was quite similar on the tree cell lines.

325 PhtFerr and its prodrug Phtester were highly toxic to U87 cells, with very low  $IC_{50}$  values of  
326  $1.6 \times 10^{-1} \mu\text{M}$  and  $9.2 \times 10^{-2} \mu\text{M}$ , respectively. The  $IC_{50}$  values for MDA-MB-231 cells were  
327 slightly higher for these compound but differences were not significant (Table 3; Kruskal  
328 Wallis, Dunn's post hoc test vs U87 :  $p > 0.05$ ).

329 The  $IC_{50}$  of PhtFerr and its prodrug Phtester were significantly higher (i.e. less toxic) on  
330 astrocytes (Table 3; Kruskal Wallis, Dunn's post hoc test vs U87:  $p < 0.05$ ). When  
331 encapsulated, the Phtester drug candidate conserved an important toxicity for glioblastoma  
332 cells.

333 Similarly, SuccFerr and its prodrug Succester were highly toxic to U87 cells, with very low  
334  $IC_{50}$  values of  $2.7 \cdot 10^{-2} \mu\text{M}$  and  $6.7 \cdot 10^{-2} \mu\text{M}$ , respectively (Table 3; Kruskal Wallis, Dunn's  
335 post hoc test vs U87:  $p < 0.05$ ). The encapsulation of Succester in LNCs or PCL-NCs did not  
336 alter or prevent the efficacy of the drug candidates on glioblastoma cells.

337 Importantly, Phtester- and Succester-loaded formulations did not alter cell viability for  
338 healthy astrocytes at the micromolar range.



339

340

### 341 **3.4.3. Cell cycle analysis**

342 The different treatments induced a major blockade in the subG1 and in S phases of the cell  
343 cycle (Figure 3) compared to their respective controls. This is in agreement with the cytotoxic  
344 activity of the different treatments (Table 3). Such an increase in the subG1 cell population  
345 revealed an alteration of the DNA content within the treated cells, which could occur either by  
346 necrosis or apoptosis.

347

### 348 **3.4.4. Cell apoptosis assay**

349 To investigate whether the native drugs candidates and their encapsulated forms induced  
350 apoptosis in U87 glioblastoma cells, we measured the induction of apoptosis with an active  
351 caspase-3 assay (Figure 4). All of the molecules and nanoformulations induced a significant  
352 increase in apoptosis after 96 h of treatment at 10  $\mu$ M. We also observed a major pro-  
353 apoptotic effect of the Phtester PCL-NC formulation. All together, these results confirmed  
354 that the increased subG1 fractions observed (Figure 3) were due to the induction of apoptosis.

355

356

#### 357 4. Discussion

358 Both PhtFerr and SuccFerr are tamoxifen derivatives and promising drug candidates for the  
359 treatment of cancer. However, these compounds are almost insoluble in water, and it is  
360 necessary to adapt their formulations to increase water solubility. Therefore, we decided to  
361 modify their chemistry by means of esterification and to encapsulate the resulting prodrugs  
362 Phtester and Succester into PCL-NCs and LNCs. Since we think that an intravenous  
363 administration of these nanocapsules could induce hepatic toxicity, we proposed these  
364 formulations for a Convection-Enhanced Delivery (CED) for further *in vivo* experiments.

365 Polyester nanocapsules (PCL-NCs) can be produced by a solvent evaporation method:  
366 polymers and drug candidates are dissolved in an organic phase (*ie* oils and volatile water-  
367 miscible solvents) constituting the inner phase of an oil-in-water emulsion (O/W). The  
368 diffusion of the organic solvent into the aqueous phase causes precipitation of the polymer at  
369 the interface, and the final nanocarriers are made of an oily core and a polymeric shell. The  
370 blank PCL-NC formulation did not show any particular toxicity in our various cell models, as  
371 indicated by the very high IC<sub>50</sub> values on normal and cancer cells (Table 3).

372

373 In the present study, loaded LNCs and PCL-NCs had different drug release kinetics. Loaded  
374 PCL-NCs released approximately 60% of the initial drug amount within 6 h. This is  
375 considered very substantial compared to the release properties of LNCs, which showed a  
376 much slower release pattern (7 and 16%, respectively, for Phtester LNCs and Succester LNCs  
377 within 6 h). Consequently, both nanocarriers and their associated release patterns could be  
378 suitable for cancer treatment delivery, allowing fast or delayed delivery, respectively.

379 Considering drug-loaded nanocapsules, the mechanisms of cytotoxicity are a complex matter.  
380 The commonest method for lipophilic drugs to pass through cell membranes is passive

381 diffusion but if the drug is included in nanocarriers, the diffusion can occur only after the  
382 release in the medium (which is in favor of a lower toxicity); simultaneously, an adsorption of  
383 the nanocarriers on the surface can induce a direct toxicity or be followed by an uptake of the  
384 particles (phagocytosis, macropinocytosis, caveolae-mediated pathways, ...). Some of these  
385 mechanisms have been reported for U87 (*eg* phagocytosis<sup>[34]</sup>) and for MDA-MB-231 (*eg*  
386 clathrin- and caveolae-mediated pathways<sup>[35]</sup>). The accurate mechanisms of uptake have not  
387 been explored in this study; nevertheless, the *in vitro* experiments conducted with the  
388 nanocapsules loaded with hydroxyferrocifens ester prodrugs (*ie* Succester and Phtester)  
389 showed more cytotoxicity in cancer cells (MDA-MB-231 and U87) than in healthy astrocytes.  
390 This important result suggests that targeting either glioblastoma cells or brain metastases from  
391 breast cancer with encapsulated esterified hydroxyferrocifens could prevent off-target toxicity  
392 to normal surrounding healthy brain tissue.

393 The anticancer activity of these Ferr derivatives encapsulated into LNCs and PCL-NCs  
394 resulted from a combination of cytostatic effects (S-phase blockade) and cytotoxic effects  
395 (induction of apoptosis).

396 Importantly, LNCs have high drug-loading capacity, long-term physical stability, and a  
397 sustained drug release pattern, and they are able to enter the intracellular compartment of  
398 epithelial or glioma cells.<sup>[36]</sup> For all of these reasons, it is widely accepted that LNCs  
399 represent one of the most promising nanoplatforms for central nervous system delivery.<sup>[36]</sup>

400

401 **5. Conclusion**

402

403 Taken together, our results indicate that the Phtester and Succester prodrugs are ferrocenyl-  
404 tamoxifen derivatives that are active against breast cancer and glioblastoma cells.

405 Encapsulation of these molecules in LNCs does not modify their anticancer properties against  
406 these cell lines, though it does increase their solubility without adding toxicity to healthy  
407 astrocytes. We postulate that these formulations could be developed for CED administration  
408 and should be further explored for cancers located in the CNS, such as brain metastases of  
409 breast cancer or glioblastoma.

410

411

412

413

414

415 **Acknowledgements:** Feten Najlaoui thanks the University of Cartage for financial support  
416 during the PhD thesis process. Michel De Waard acknowledges financial support from  
417 Inserm.

418

419 **Conflict of interest:** The authors claim that no conflict of interest, financial or otherwise.

420

421  
422  
423  
424

**Table 1:** Solubility of Phtester and Succester in various oils and surfactants

<b>Vehicle</b>	<b>HLB*</b>	<b>Solubility of Phtester (mg/mL)</b>	<b>Solubility of Succester (mg/mL)</b>
Tween® 20	16.7	408 ± 12	312 ± 15
Tween® 20 - 1%	16.7	1.2	6.2
Tween® 20 - 5%	16.7	15	19
Tween® 20 - 10%	16.7	26	15
Tween® 20 - 20%	16.7	43	29
Tween® 80	15	532 ± 8	619 ± 56
Solutol® HS 15	14-16	309 ± 61	408 ± 12
Labrasol® ALF	12	10.0 ± 0.1	11 ± 1
Triethylcitrate	8.1	660 ± 17	432 ± 38
Capryol® 90	6	3.8 ± 0.1	1.4 ± 0.1
Transcutol® HP	4.2	39 ± 0.1	20 ± 3
Maisine® 35-1	4	6.0x10 <sup>-2</sup> ± 0.1x10 <sup>-2</sup>	1.2 ± 0.1
Miglyol® 812	15.4	7.2x10 <sup>-4</sup> ± 0.8x10 <sup>-4</sup>	6.1x10 <sup>-4</sup> ± 0.1x10 <sup>-4</sup>
Labrafac®	6	460 ± 5	465 ± 12
Benzoate benzyle	1	0.32 ± 0.01	2.0 ± 0.6
Triacetin®	Oil	5.7 ± 0.4	8.2 ± 0.2
Ethyl oleate	Oil	9.1x10 <sup>-4</sup> ± 0.6x10 <sup>-4</sup>	11.10 <sup>-4</sup> ± 1.10 <sup>-4</sup>
Captex® 355	Oil	9.3 ± 0.1	8.5 ± 0.1
Olive oil	Oil	6.1x10 <sup>-2</sup> ± 0.1x10 <sup>-2</sup>	0.5x10 <sup>-3</sup> ± 0.03x10 <sup>-3</sup>

425 \* HLB: Hydrophilic Lipophilic Balance

426

427  
428  
429  
430  
431  
432  
433

**Table 2:** Mean characterization of the different nanocarriers formulations

	<b>Mean particle size (nm)</b>	<b>Polydispersity index (PI)</b>	<b>Zeta potential (mV)</b>	<b>Drug load (mg/g)</b>	<b>Encapsulation yield (%)</b>
<b>Blank LNC</b>	50.3 ± 0.2	0.071 ± 0.003	-8.9 ± 1.2	-	-
<b>Phtester LNC</b>	53.4 ± 0.9	0.134 ± 0.005	-10.8 ± 2.0	2.5 ± 0.6	94 ± 3
<b>Sucester LNC</b>	57.8 ± 2.0	0.118 ± 0.009	-11.1 ± 1.3	3.1 ± 0.2	92 ± 6
<b>Blank PCL-NC</b>	289 ± 7.0	0.248 ± 0.011	-13.8 ± 0.5	-	-
<b>Phtester PCL-NC</b>	303 ± 12	0.323 ± 0.003	-18.2 ± 0.7	9.0 ± 1.1	72 ± 6
<b>Sucester PCL-NC</b>	295 ± 18	0.267 ± 0.006	-14.9 ± 2.4	7.3 ± 0.4	81 ± 2

434 Measurements were made in triplicates (n= 3) and results were expressed as mean values ± SD. Experimental drug load were  
435 expressed as the amount of drug in milligrams per gram of lipid nanocapsules suspension. Encapsulation efficiency was  
436 expressed as mean percentage (%) ± SD.

437  
438  
439  
440

441

442 **Table 3:** Cytotoxicity ( $IC_{50}$ ) of the indicated drugs on astrocytes, MDA-MB-231 and U87 cells.

443

<b><math>IC_{50}(\mu M)</math> [95% CI]</b>			
	<b>Astrocytes</b>	<b>MDA-MB-231</b>	<b>U87</b>
Blank PCL-NC	$7.4 \cdot 10^2$ [ $1.4 \cdot 10^2$ - $9.6 \cdot 10^3$ ]	$1.8 \cdot 10^2$ [ $0.6 \cdot 10^2$ - $2.7 \cdot 10^3$ ]	$4.0 \cdot 10^3$ [ $2.6 \cdot 10^3$ - $1.2 \cdot 10^4$ ]
Blank LNC	$7.6 \cdot 10^2$ [ $1.9$ - $2.2 \cdot 10^3$ ]	$3.0 \cdot 10^1$ [ $6.3$ - $2.3 \cdot 10^2$ ]	$6.0 \cdot 10^3$ [ $8.8 \cdot 10^1$ - $1.2 \cdot 10^4$ ]
PhtFerr	$3.7 \cdot 10^1$ [ $1.3 \cdot 10^1$ - $3.3 \cdot 10^2$ ]	$2.0 \cdot 10^1$ [ $1.3 \cdot 10^2$ - $2.3 \cdot 10^{-1}$ ]	$1.6 \cdot 10^{-1}$ [ $3.8 \cdot 10^{-2}$ - $2.2 \cdot 10^{-1}$ ]
Phtester	$7.8 \cdot 10^2$ [ $1.0$ - $7.1 \cdot 10^3$ ]	1.0 [0.28-5.6]	$9.2 \cdot 10^{-2}$ [ $3.8 \cdot 10^{-2}$ - $2.2 \cdot 10^{-1}$ ]
Phtester-LNC	$8.0 \cdot 10^2$ [ $2.1 \cdot 10^2$ - $2.1 \cdot 10^3$ ]	$2.1 \cdot 10^1$ [ $2.1$ - $1.8 \cdot 10^2$ ]	$7.0 \cdot 10^{-2}$ [ $2.1 \cdot 10^{-2}$ - $2.3 \cdot 10^{-1}$ ]
Phtester PCL-NC	$6.8 \cdot 10^2$ [ $1.1 \cdot 10^2$ - $7.3 \cdot 10^2$ ]	$4.6 \cdot 10^1$ [ $5.1$ - $2.4 \cdot 10^2$ ]	$7.6 \cdot 10^{-2}$ [ $2.1 \cdot 10^{-2}$ - $2.3 \cdot 10^{-1}$ ]
SuccFerr	$3.4 \cdot 10^1$ [ $6.3$ - $7.5 \cdot 10^1$ ]	$3.3 \cdot 10^{-1}$ [ $4.7 \cdot 10^{-2}$ -1.0]	$2.7 \cdot 10^{-2}$ [ $6.7 \cdot 10^{-3}$ - $1.1 \cdot 10^{-1}$ ]
Sucester	$7.1 \cdot 10^2$ [ $2.1 \cdot 10^2$ - $1.0 \cdot 10^3$ ]	$6.0 \cdot 10^{-1}$ [ $1.3 \cdot 10^{-1}$ - $9.4 \cdot 10^{-1}$ ]	$6.7 \cdot 10^{-2}$ [ $1.3 \cdot 10^{-2}$ - $3.4 \cdot 10^{-2}$ ]
Sucester LNC	$7.0 \cdot 10^2$ [ $1.2 \cdot 10^2$ - $8.1 \cdot 10^2$ ]	$1.8 \cdot 10^1$ [ $1.5 \cdot 10^1$ - $1.4 \cdot 10^2$ ]	$4.6 \cdot 10^{-2}$ [ $1.5 \cdot 10^{-2}$ - $1.4 \cdot 10^{-1}$ ]
Sucester-PCL-NC	$7.8 \cdot 10^2$ [ $3.3 \cdot 10^2$ - $4.2 \cdot 10^3$ ]	$2.0 \cdot 10^1$ [ $1.2 \cdot 10^1$ - $2.7 \cdot 10^1$ ]	$5.7 \cdot 10^{-2}$ [ $1.2 \cdot 10^{-2}$ - $2.7 \cdot 10^{-1}$ ]
Tamoxifen	1.85 [0.94-3.62]	2,63 [0.39-17.94]	1.92 [0.57-6.38]

444

445



446 **References**

447

- 448 1. Jordan VC. Antiestrogens and selective estrogen receptor modulators as  
449 multifunctional medicines. 1. Receptor interactions. *J Med Chem* 2003; 6: 883-908.
- 450 2. Fan P, Craig Jordan V. Acquired resistance to selective estrogen receptor modulators  
451 (SERMs) in clinical practice (tamoxifen & raloxifene) by selection pressure in breast  
452 cancer cell populations. *Steroids* 2014: 44-52.
- 453 3. Di Cristofori A *et al.* Continuous tamoxifen and dose-dense temozolomide in recurrent  
454 glioblastoma. *Anticancer Res* 2013; 8: 3383-3389.
- 455 4. Jaouen G *et al.* The first organometallic selective estrogen receptor modulators  
456 (SERMs) and their relevance to breast cancer. *Curr Med Chem* 2004; 18: 2505-2517.
- 457 5. Top S *et al.* Synthesis, Biochemical Properties and Molecular Modelling Studies of  
458 Organometallic Specific Estrogen Receptor Modulators (SERMs), the Ferrocifens and  
459 Hydroxyferrocifens: Evidence for an Antiproliferative Effect of Hydroxyferrocifens  
460 on both Hormone-Dependent and Hormone-Independent Breast Cancer Cell Lines.  
461 *Chemistry* 2003; 21: 5223-5236.
- 462 6. Jaouen G *et al.* Ferrocifen type anti cancer drugs. *Chem Soc Rev* 2015; 24: 8802-8817.
- 463 7. Richard MA *et al.* Oxidative metabolism of ferrocene analogues of tamoxifen:  
464 characterization and antiproliferative activities of the metabolites. *Chem Med Chem*  
465 2015; 6: 981-990.
- 466 8. Wang Y *et al.* Organometallic Antitumor Compounds: Ferrocifens as Precursors to  
467 Quinone Methides. *Angew Chem Int Ed Engl* 2015; 35: 10230-10233.

- 468 9. Najlaoui F *et al.* Phthalimido-ferrocenylphenol cyclodextrin complexes:  
469 Characterization and anticancer activity. *Int J Pharm* 2015; 1-2: 323-334.
- 470 10. Bruyere C *et al.* Ferrocifen derivatives that induce senescence in cancer cells: selected  
471 examples. *Journal of Inorganic Biochemistry* 2014: 144-151.
- 472 11. Citta A *et al.* Evidence for targeting thioredoxin reductases with ferrocenyl quinone  
473 methides. A possible molecular basis for the antiproliferative effect of  
474 hydroxyferrocifens on cancer cells. *J Med Chem* 2014; 21: 8849-8859.
- 475 12. Wang Y *et al.* Ferrocenyl quinone methide-thiol adducts as new antiproliferative  
476 agents: synthesis, metabolic formation from ferrocenophenols and oxidative  
477 transformation. *Angew Chem Int Ed* 2016; 35.
- 478 13. Laine AL, Passirani C. Novel metal-based anticancer drugs: a new challenge in drug  
479 delivery. *Curr Opin Pharmacol* 2012; 4: 420-426.
- 480 14. Huynh NT *et al.* Lipid nanocapsules: a new platform for nanomedicine. *Int J Pharm*  
481 2009; 2: 201-209.
- 482 15. Allard E *et al.* Dose effect activity of ferrocifen-loaded lipid nanocapsules on a 9L-  
483 glioma model. *Int J Pharm* 2009; 2: 317-323.
- 484 16. David S *et al.* Treatment efficacy of DNA lipid nanocapsules and DNA multimodular  
485 systems after systemic administration in a human glioma model. *J Gene Med* 2012;  
486 12: 769-775.
- 487 17. David S *et al.* siRNA LNCs--a novel platform of lipid nanocapsules for systemic  
488 siRNA administration. *Eur J Pharm Biopharm* 2012; 2: 448-452.

- 489 18. Vanpouille-Box C *et al.* Tumor eradication in rat glioma and bypass of  
490 immunosuppressive barriers using internal radiation with (188)Re-lipid nanocapsules.  
491 *Biomaterials* 2011; 28: 6781-6790.
- 492 19. Vanpouille-Box C *et al.* Lipid nanocapsules loaded with rhenium-188 reduce tumor  
493 progression in a rat hepatocellular carcinoma model. *PloS one* 2011; 3: e16926.
- 494 20. Griveau A *et al.* Silencing of miR-21 by locked nucleic acid-lipid nanocapsule  
495 complexes sensitize human glioblastoma cells to radiation-induced cell death. *Int J*  
496 *Pharm* 2013; 2: 765-774.
- 497 21. Letchford K, Burt H. A review of the formation and classification of amphiphilic  
498 block copolymer nanoparticulate structures: micelles, nanospheres, nanocapsules and  
499 polymersomes. *Eur J Pharm Biopharm* 2007; 3: 259-269.
- 500 22. Ali SAM *et al.* Mechanisms of polymer degradation in implantable devices. I.  
501 Poly(caprolactone). *Biomaterials* 1993; 9: 648-656.
- 502 23. Yang X *et al.* In vitro and in vivo safety evaluation of biodegradable self-assembled  
503 monomethyl poly (ethylene glycol)-poly (epsilon-caprolactone)-poly (trimethylene  
504 carbonate) micelles. *J Pharm Sci* 2014; 1: 305-313.
- 505 24. Nga VD *et al.* Effects of polycaprolactone-based scaffolds on the blood-brain barrier  
506 and cerebral inflammation. *Tissue Eng Part A* 2015; 3-4: 647-653.
- 507 25. Minick DJ *et al.* A comprehensive method for determining hydrophobicity constants  
508 by reversed-phase high-performance liquid chromatography. *J Med Chem* 1988; 10:  
509 1923-1933.

- 510 26. Heurtault B *et al.* A novel phase inversion-based process for the preparation of lipid  
511 nanocarriers. *Pharm Res* 2002; 6: 875-880.
- 512 27. McCarthy KD, de Vellis J. Preparation of separate astroglial and oligodendroglial cell  
513 cultures from rat cerebral tissue. *J Cell Biol* 1980; 3: 890-902.
- 514 28. Heurtault B *et al.* The influence of lipid nanocapsule composition on their size  
515 distribution. *Eur J Pharm Sci* 2003; 1: 55-61.
- 516 29. Vonarbourg A *et al.* Evaluation of pegylated lipid nanocapsules versus complement  
517 system activation and macrophage uptake. *J Biomed Mater Res A* 2006; 3: 620-628.
- 518 30. Vonarbourg A *et al.* Electrokinetic properties of noncharged lipid nanocapsules:  
519 influence of the dipolar distribution at the interface. *Electrophoresis* 2005; 11: 2066-  
520 2075.
- 521 31. Lamprecht A *et al.* New lipid nanocapsules exhibit sustained release properties for  
522 amiodarone. *J Control Release* 2002; 1-2: 59-68.
- 523 32. Malzert-Freon A *et al.* Formulation of sustained release nanoparticles loaded with a  
524 triptentone, a new anticancer agent. *Int J Pharm* 2006; 1-2: 157-164.
- 525 33. Peltier S *et al.* Enhanced oral paclitaxel bioavailability after administration of  
526 paclitaxel-loaded lipid nanocapsules. *Pharm Res* 2006; 6: 1243-1250.
- 527 34. Li Y *et al.* Mechanisms of U87 astrocytoma cell uptake and trafficking of monomeric  
528 versus protofibril Alzheimer's disease amyloid-beta proteins. *PloS one* 2014; 6:  
529 e99939.

530 35. Xu R *et al.* An injectable nanoparticle generator enhances delivery of cancer  
531 therapeutics. *Nat Biotechnol* 2016; 4: 414-418.

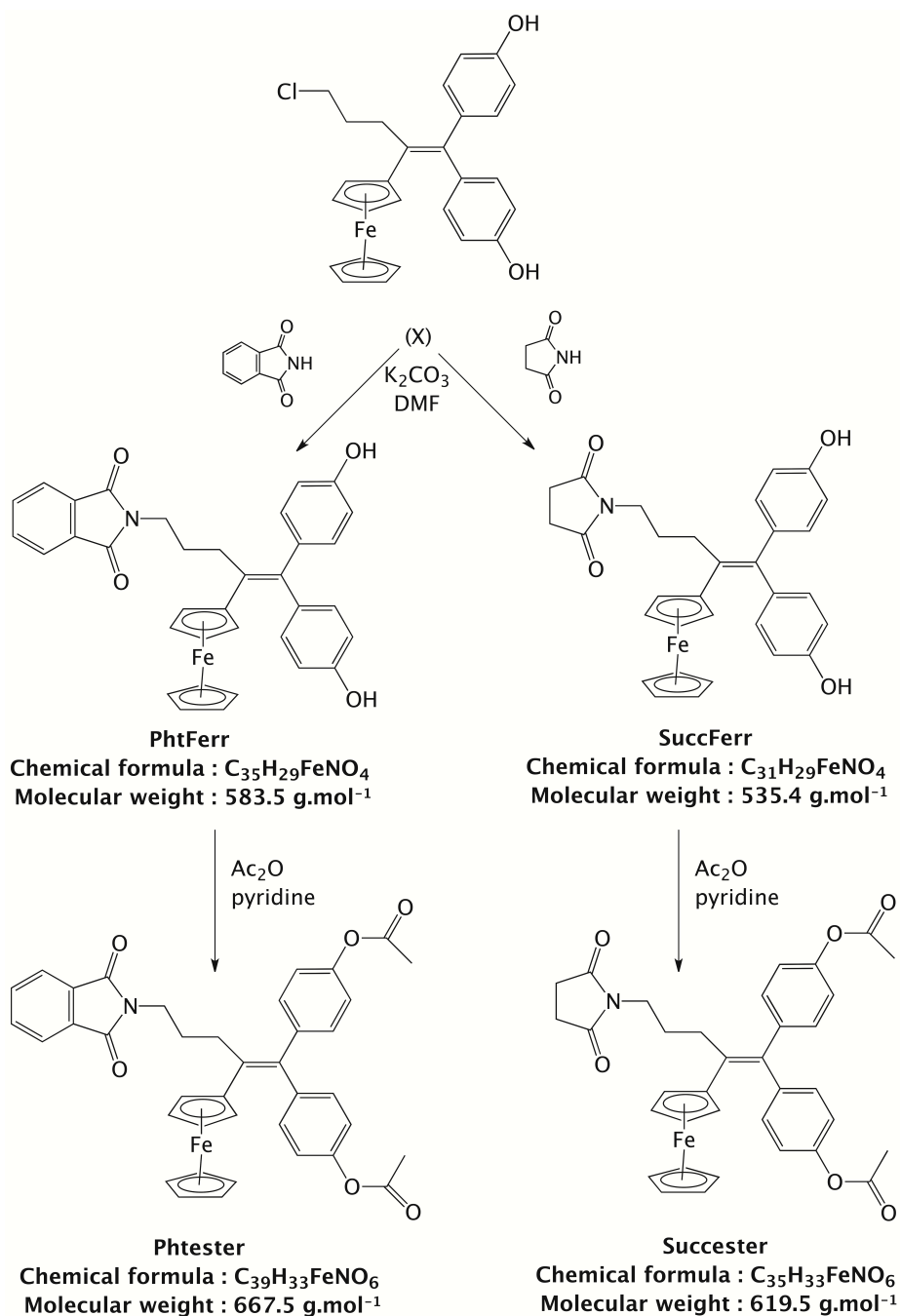
532 36. Aparicio-Blanco J, Torres-Suárez A-I. Glioblastoma Multiforme and Lipid  
533 Nanocapsules: A Review. *J Biomed Nanotechnol* 2015; 8: 1283-1311.

534

535

536 **Figure 1.** Chemical structure and synthesis of the main compounds: Phthalimido-ester (**Phtester**) and  
 537 Succinimido-ester (**Succester**) by acetylation of **PhtFerr** and **SuccFerr**. Synthesis of these precursors  
 538 by substitution reaction on the chlorinated alkene **X** using phthalimide or succinimide.

539



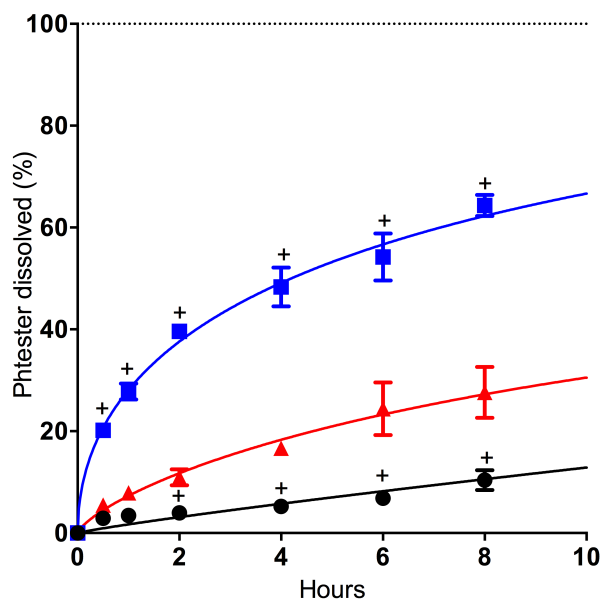
540

541

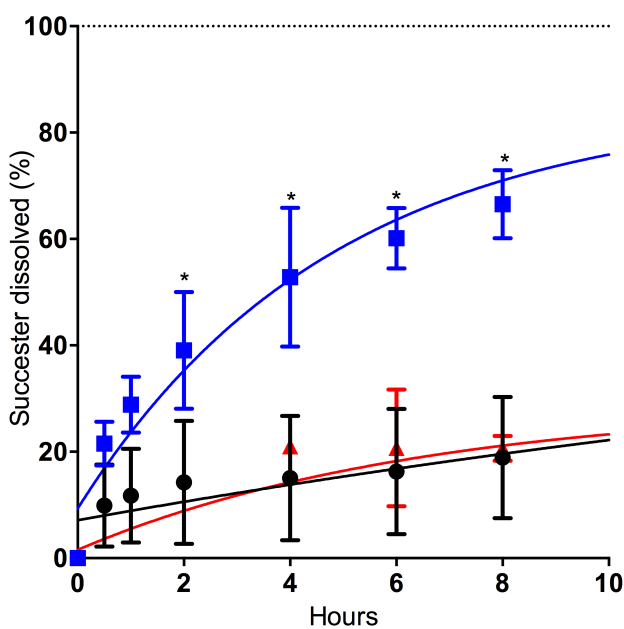
542

543 **Figure 2.** Release profiles of a) Phtester [from Phtester (-▲-), Phtester LNC (-●-), Phtester PCL-NC  
 544 (-■-)] and b) Succester [from Succester (-▲-), Succester LNC (-●-), and Succester PCL-NC (-■-)] by  
 545 dialysis in Tween<sup>®</sup> 20 (1%) ; + different vs Phtester, p < 0.05 (Mann and Whitney) ; \* different vs  
 546 Succester, p < 0.05 (Mann and Whitney).

547



548



549

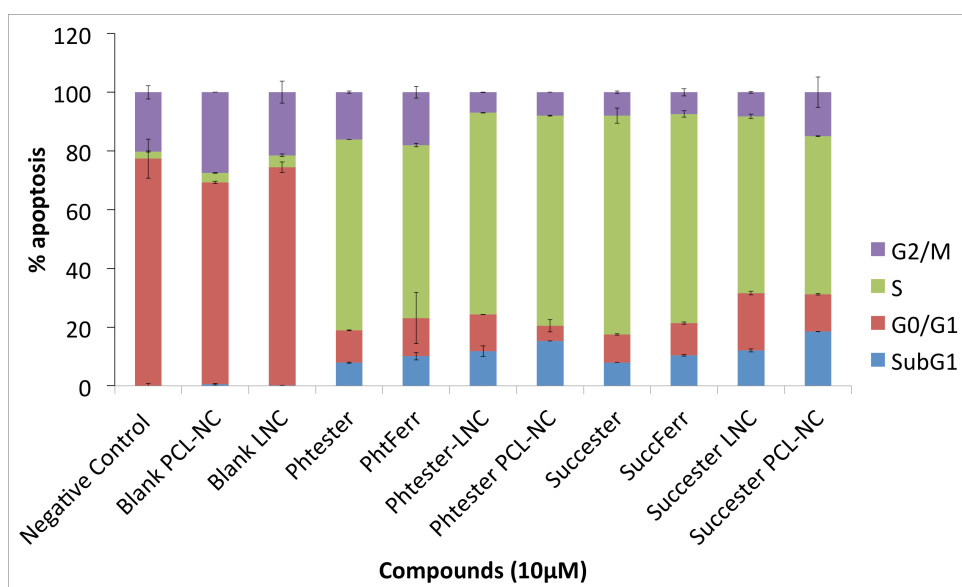
550

551

552

**Figure 3. Cell cycle distribution**

553



554

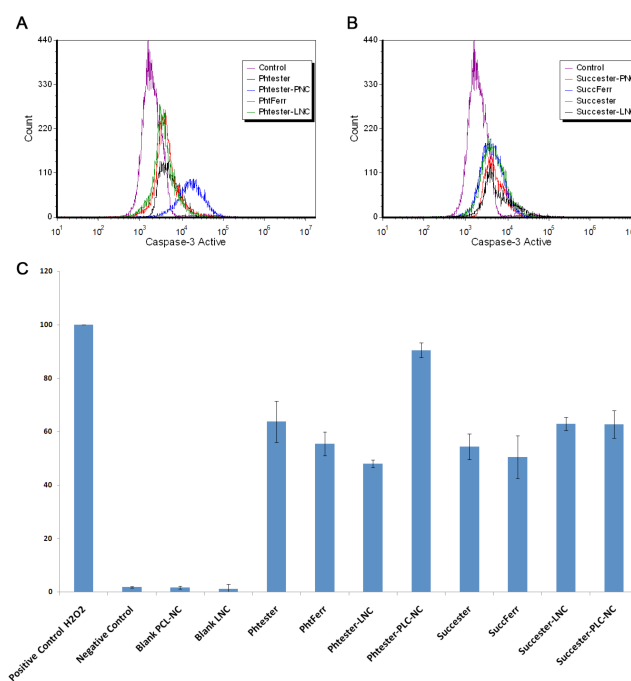
555

**Figure 4. Apoptosis counting (panel a-b) and percentage of caspase-3 active cells (panel c) after 96 h of treatment**

556

557

558



559



## 560 **Supplementary Materials for the Chemistry Section:**

### 561 **Chemical Reagents**

562

563 The starting materials for the synthesis were acetic anhydride, pyridine, hydrochloric acid,  
564 sodium hydroxide, tetrahydrofuran (THF) magnesium sulfate, cyclohexane and ethyl acetate  
565 which were obtained from Sigma–Aldrich (L’Isle d’Abeau Chesnes, 38297 Saint-Quentin,  
566 Fallavier, France), TCI EUROPE N.V. (Boerenveldseweg 6, Haven 1063, 2070 Zwijndrecht,  
567 Belgique), and Alfa Aesar France (2 allée d’Oslo, 67300 Schiltigheim, France).

568 All reactions and manipulations were carried out under an argon atmosphere using standard  
569 Schlenk techniques. THF was distilled over sodium/benzophenone prior to use. Thin layer  
570 chromatography was performed on silica gel 60 GF<sub>254</sub>. IR spectra were obtained on a FT/IR-  
571 4100 JASCO 180 spectrometer. <sup>1</sup>H and <sup>13</sup>C NMR spectra were acquired on a Bruker 300  
572 MHz spectrometer. Mass spectrometry was carried out at the “Service de Spectrométrie de  
573 Masse” at ENSCP, Paris. High-resolution mass spectra (HRMS) were acquired in the “Institut  
574 Parisien de Chimie Moléculaire (IPCM – UMR 8232)” at the “Université Pierre et Marie  
575 Curie”, Paris. Microanalyses were performed by the “Service de Microanalyse ICSN” at Gif  
576 sur Yvette, France. We already described the synthesis of **PhtFerr** compounds elsewhere (7).  
577 Measurements of the octanol/water partition coefficient (log Po/w) were made by the HPLC  
578 technique according to a method described previously (see ref 21). Measurement of the  
579 chromatographic capacity factors (k) for each molecule was done at various concentrations in  
580 the range of 95–75% methanol containing 0.25% (v/v) 1-octanol and an aqueous phase  
581 consisting of 0.15% (v/v) n-decylamine in the buffering agent MOPS (3-morpholinopropane-  
582 1-sulfonic acid, prepared in 1-octanol saturated water) adjusted to pH 7.4. These capacity  
583 factors (k’) are extrapolated to 100% of the aqueous component given the value of k’<sub>w</sub>. The  
584 log Po/w is obtained by the formula  $\log Po/w = 0.13418 + 0.98452 \log k'$ .

585

586 The lipophilic Labrafac® CC (caprylic/capric acid triglycerides) was provided by Gattefosse  
587 S.A. (Saint-Priest, France). Lipoïd® S75-3 (soybean lecithin at 69% of phosphatidylcholine)  
588 was a gift from Lipoïd GmbH (Ludwigshafen, Germany); Solutol® HS15 (a mixture of free  
589 polyethylene glycol 660 and polyethylene glycol 660 hydroxystearate) was from Sigma-  
590 Aldrich (Saint Quentin Fallavier, France). Other reactants were obtained from Prolabo

591 (Fontenay-sous-bois, France). Deionised water was obtained from a Milli-Q plus system  
592 (Millipore, Paris, France).

593 Poly( $\epsilon$ -caprolactone) (PCL), triethylcitrate and Pluronic (F 68 or F 127) were purchased from  
594 Sigma-Aldrich (Saint-Quentin Fallavier, France). Egg lecithin was obtained from VWR  
595 (Fontenais-sous-Bois, France), Dulbecco modified Eagle medium (DMEM) with glucose and  
596 l-glutamine (Cergy-Pontoise, France), foetal calf serum (FCS) (BioWhittaker) and antibiotic  
597 and antimycotic solution (Sigma, Saint-Quentin Fallavier, France).

598

### 599 **Synthesis of SuccFerr :**

#### 600 ***N*-{4-ferrocenyl-5,5-bis-(4-hydroxyphenyl)-pent-4-enyl}succinimide (SuccFerr):**

601 A mixture of potassium carbonate (0.478 g, 3.5 mmoles) and succinimide (0.457 g, 4.6  
602 mmoles) in dimethylformamide (DMF) was heated at 80°C for 15 min. The compound **X** (5-  
603 chloro-2-ferrocenyl-1,1-bis-(4-hydroxyphenyl)-pent-1-ene, 1.09 g, 2.31 mmoles) was added  
604 and the stirring was continued at 80°C overnight. The mixture was allowed to cool to room  
605 temperature, was poured into a diluted hydrochloric acid solution, was extracted twice with  
606 diethyl ether, then the organic layer was dried on magnesium sulfate and concentrated under  
607 reduced pressure. The residue was purified by flash-chromatography (ethyl acetate) to afford  
608 the imide **SuccFerr** that was obtained as an orange solid with a yield of 54% (0.662 g). mp:  
609 225°C decomp. The corresponding NMR profile is described hereafter in the mass  
610 spectrometry section.

611

### 612 **Synthesis of Phtester:**

#### 613 ***N*-{4-ferrocenyl-5,5-bis-(4-acetoxyphenyl)-pent-4-enyl}phthalimide (Phtester):**

614 Acetic anhydride (10 mL) was added dropwise to a solution of PhtFerr (3.01 g, 5.16 mmol)  
615 and pyridine (1.63 g, 1.7 mL, 20.6 mmol) in dry THF (50 mL) at RT then the reaction mixture  
616 was stirred at RT overnight. The solution was then poured into water (300 mL) in presence of  
617 hydrochloric acid (10 mL) and dichloromethane (300 mL) and the layers were separated. The  
618 aqueous layer was extracted twice with dichloromethane and the combined organic layers  
619 were washed with a solution of sodium hydroxide (2 g in 300 mL of water), then with water.  
620 The solution was dried over magnesium sulfate and concentrated under reduced pressure.

621 Flash chromatography (cyclohexane/ethyl acetate 1/1) then recrystallization from ethyl  
622 acetate yielded the pure product as an orange solid (2.87 g, 84 %). Mp: 210°C. The  
623 corresponding NMR profile is described hereafter in the mass spectrometry section. The  
624 partition coefficient of the obtained **Phtester** was the following: Log Po/w: 6.09. This  
625 corresponds to a high hydrophobicity profile.

626

#### 627 **Synthesis of Succester:**

##### 628 ***N*-{4-ferrocenyl-5,5-bis-(4-acetoxyphenyl)-pent-4-enyl}succinimide (Succester):**

629 Acetic anhydride (18 mL) was added dropwise to a solution of SuccFerr (5 g, 9.34 mmol) and  
630 pyridine (2.95 g, 3.1 mL, 37.3 mmol) in dry THF (80 mL) at RT then the reaction mixture  
631 was stirred at RT overnight. The solution was then poured into water (400 mL) in addition to  
632 hydrochloric acid (15 mL) and dichloromethane (400 mL) and the layers were separated. The  
633 aqueous layer was extracted twice with dichloromethane and the combined organic layers  
634 were washed with a solution of sodium hydroxide (3 g in 400 mL of water), then with water.  
635 The solution was dried over magnesium sulfate and concentrated under reduced pressure.  
636 Flash chromatography (cyclohexane/ethyl acetate 1/1) then recrystallization from ethyl  
637 acetate yielded the pure product as an orange solid (5.3 g, 92 %). Mp: 157°C. The  
638 corresponding NMR profile is described hereafter in the mass spectrometry section. The  
639 partition coefficient of the obtained **Succester** was the following: Log Po/w: 5.18. This  
640 corresponds to a high hydrophobicity profile.

641

#### 642 **Mass spectrometry: characterization of the products**

##### 643 ***N*-{4-ferrocenyl-5,5-bis-(4-hydroxyphenyl)-pent-4-enyl}succinimide (SuccFerr):**

644 <sup>1</sup>H NMR (300 MHz, acetone-d<sub>6</sub>) : δ 1.70-1.81 (m, 2H, CH<sub>2</sub>), 2.56-2.64 (m, 6H, 2CH<sub>2</sub>  
645 succ+CH<sub>2</sub>-C=C), 3.38 (t, *J* = 6.6 Hz, 2H, CH<sub>2</sub>N), 3.95 (t, *J* = 1.9 Hz, 2H, C<sub>5</sub>H<sub>4</sub>), 4.10 (t, *J* =  
646 1.9 Hz, 2H, C<sub>5</sub>H<sub>4</sub>), 4.16 (s, 5H, Cp), 6.74 (d, *J* = 8.6 Hz, 2H, C<sub>6</sub>H<sub>4</sub>), 6.85 (d, *J* = 8.6 Hz, 2H,  
647 C<sub>6</sub>H<sub>4</sub>), 6.91 (d, *J* = 8.6 Hz, 2H, C<sub>6</sub>H<sub>4</sub>), 7.04 (d, *J* = 8.6 Hz, 2H, C<sub>6</sub>H<sub>4</sub>), 8.25 (s, 1H, OH), 8.36  
648 (s, 1H, OH). <sup>13</sup>C NMR (75 MHz, acetone-d<sub>6</sub>) : δ 29.4 (2CH<sub>2</sub>, succinimide), 30.8 (CH<sub>2</sub>), 33.8  
649 (CH<sub>2</sub>), 39.7 (CH<sub>2</sub>), 69.5 (2CH, C<sub>5</sub>H<sub>4</sub>), 70.7 (5CH, Cp+2CH, C<sub>5</sub>H<sub>4</sub>), 88.8 (C, C<sub>5</sub>H<sub>4</sub>), 116.5  
650 (2CH, C<sub>6</sub>H<sub>4</sub>), 116.6 (2CH, C<sub>6</sub>H<sub>4</sub>), 132.0 (2CH, C<sub>6</sub>H<sub>4</sub>), 132.4 (2CH, C<sub>6</sub>H<sub>4</sub>), 135.3 (C), 137.7

651 (C), 137.9 (C), 140.2 (C), 157.3 (C), 157.5 (C), 178.6 (2CO). IR (KBr,  $\nu$   $\text{cm}^{-1}$ ): 3421 (OH),  
652 3096, 2967, 2936 (CH, CH<sub>2</sub>), 1697 (CO). MS (ESI)  $m/z$ : 535 [M]<sup>+</sup>, 342, 279, 224, 143, 83.  
653 HRMS (ESI, C<sub>31</sub>H<sub>29</sub>FeNO<sub>4</sub>: [M]<sup>+</sup>) calcd: 535.1446, found: 535.1460. Anal. Calcd for  
654 C<sub>31</sub>H<sub>29</sub>FeNO<sub>4</sub>(H<sub>2</sub>O)<sub>0.3</sub>: C, 68.85; H, 5.51; N, 2.58. Found: C, 68.76; H, 5.14; N, 2.37.

655 ***N*-{4-ferrocenyl-5,5-bis-(4-acetoxyphenyl)-pent-4-enyl}phthalimide (Phtester):**

656 <sup>1</sup>H NMR (DMSO-d<sub>6</sub>):  $\delta$  1.70-1.89 (m, 2H, CH<sub>2</sub>), 2.24 (s, 6H, Me), 2.42-2.49 (m, 2H, CH<sub>2</sub>),  
657 3.50 (t,  $J$  = 6.4 Hz, 2H, CH<sub>2</sub>N), 3.79 (t,  $J$  = 1.7 Hz, 2H, C<sub>5</sub>H<sub>4</sub>), 4.10 (s, 7H, Cp + C<sub>5</sub>H<sub>4</sub>), 6.89  
658 (d,  $J$  = 8.5 Hz, 2H, C<sub>6</sub>H<sub>4</sub>), 7.02 (d,  $J$  = 8.8 Hz, 2H, C<sub>6</sub>H<sub>4</sub>), 7.06 (d,  $J$  = 8.8 Hz, 2H, C<sub>6</sub>H<sub>4</sub>), 7.16  
659 (d,  $J$  = 8.5 Hz, 2H, C<sub>6</sub>H<sub>4</sub>), 7.86 (s, 4H, phthalimide). <sup>13</sup>C NMR (DMSO-d<sub>6</sub>):  $\delta$  20.8 (2CH<sub>3</sub>),  
660 29.3 (CH<sub>2</sub>), 31.5 (CH<sub>2</sub>), 37.3 (CH<sub>2</sub>), 68.2 (2CH, C<sub>5</sub>H<sub>4</sub>), 68.7 (2CH, C<sub>5</sub>H<sub>4</sub>), 69.1 (5CH, Cp),  
661 85.3 (C, C<sub>5</sub>H<sub>4</sub>), 121.4 (2CH, C<sub>6</sub>H<sub>4</sub>), 121.7 (2CH, C<sub>6</sub>H<sub>4</sub>), 122.9 (2CH, phthalimide), 129.5  
662 (2CH, C<sub>6</sub>H<sub>4</sub>), 130.1 (2CH, C<sub>6</sub>H<sub>4</sub>), 131.4 (2C, phthalimide), 134.3 (2CH, phthalimide), 135.4  
663 (C), 136.2 (C), 140.9 (C), 141.4 (C), 148.7 (C), 148.9 (C), 167.8 (2CO, phthalimide), 168.8  
664 (COO), 169.0 (COO). IR (KBr,  $\nu$   $\text{cm}^{-1}$ ): 3454 (OH), 1766, 1752, 1708 (CO). HRMS (ESI,  
665 C<sub>39</sub>H<sub>33</sub>FeNNaO<sub>6</sub>: [M+Na]<sup>+</sup>) calcd: 690.154948, found: 690.15422.

666 ***N*-{4-ferrocenyl-5,5-bis-(4-acetoxyphenyl)-pent-4-enyl}succinimide (Sucester):**

667 <sup>1</sup>H NMR (acetone-d<sub>6</sub>):  $\delta$  1.68-1.85 (m, 2H, CH<sub>2</sub>), 2.23 (s, 3H, CH<sub>3</sub>), 2.27 (s, 3H, CH<sub>3</sub>), 2.50-  
668 2.66 (m, 6H, 2CH<sub>2</sub>succinimide + CH<sub>2</sub>-C=C), 3.37 (t,  $J$  = 6.5 Hz, 2H, CH<sub>2</sub>N), 3.91 (s, 2H,  
669 C<sub>5</sub>H<sub>4</sub>), 4.11 (s, 2H, C<sub>5</sub>H<sub>4</sub>), 4.15 (s, 5H, Cp), 7.01 (d,  $J$  = 8.2 Hz, 2H, C<sub>6</sub>H<sub>4</sub>), 7.11 (d,  $J$  = 8.2  
670 Hz, 2H, C<sub>6</sub>H<sub>4</sub>), 7.12 (d,  $J$  = 8.2 Hz, 2H, C<sub>6</sub>H<sub>4</sub>), 7.26 (d,  $J$  = 8.2 Hz, 2H, C<sub>6</sub>H<sub>4</sub>). <sup>13</sup>C NMR  
671 (acetone-d<sub>6</sub>):  $\delta$  21.00 (CH<sub>3</sub>), 21.03 (CH<sub>3</sub>), 28.7 (2CH<sub>2</sub>, succinimide), 29.8 (CH<sub>2</sub>), 33.1 (CH<sub>2</sub>),  
672 38.9 (CH<sub>2</sub>), 69.2 (2CH, C<sub>5</sub>H<sub>4</sub>), 70.1 (5CH, Cp + 2CH, C<sub>5</sub>H<sub>4</sub>), 86.9 (C, C<sub>5</sub>H<sub>4</sub>), 122.5 (2CH,  
673 C<sub>6</sub>H<sub>4</sub>), 122.6 (2CH, C<sub>6</sub>H<sub>4</sub>), 131.0 (2CH, C<sub>6</sub>H<sub>4</sub>), 131.4 (2CH, C<sub>6</sub>H<sub>4</sub>), 137.1 (C), 137.7 (C),  
674 142.5 (C), 142.8 (C), 150.4 (C), 150.5 (C), 169.5 (COO), 169.7 (COO), 177.9 (2CO). IR  
675 (KBr,  $\nu$   $\text{cm}^{-1}$ ): 3443 (OH), 1764, 1752, 1697 (CO). HRMS (ESI, C<sub>35</sub>H<sub>33</sub>FeNNaO<sub>6</sub>: [M+Na]<sup>+</sup>)  
676 calcd: 642.154948, found: 642.15387. Anal. Calcd for C<sub>35</sub>H<sub>33</sub>FeNO<sub>6</sub>(H<sub>2</sub>O)<sub>0.5</sub>: C, 66.88; H,  
677 5.44; N, 2.23. Found: C, 67.26; H, 5.36; N, 2.09.

678

679